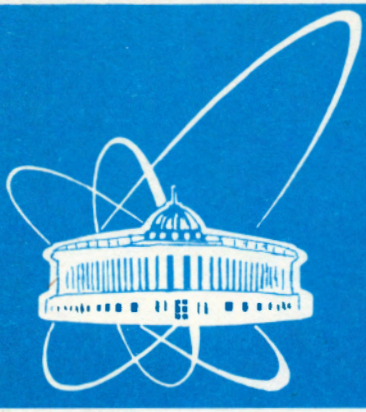

ОБЪЕДИНЕННЫЙ
ИНСТИТУТ
ЯДЕРНЫХ
ИССЛЕДОВАНИЙ

Дубна

98-287

E2-98-287

Yu.N.Uzikov

STRUCTURE OF THE ^{3}He IN BACKWARD ELASTIC $p\,^3$He-SCATTERING

Submitted to «Nuclear Physics A»

1998

1 Introduction

Owing to high momentum transfers $\Delta > 1$ GeV/c in backward elastic scattering of protons from deuteron, ^3He and ^4He nuclei at initial proton kinetic energies about of 1 GeV, the experimental data on these processes contain in principle an information on the structure of the lightest nuclei at short NN-distances in the region of nucleon overlap, $r_{NN} \sim 1/\Delta \leq 0.5$fm. However theoretical analysis performed most carefully in the simplest case of the backward elastic pd scattering [1] - [6], has not yet given quantitative results on the deuteron structure at short relative distances between the neutron and the proton, in particularly, on relativistic [6] and NN^*- components [5] of the deuteron wave function. It seems likely that this fact is connected to the extremely small binding energy of the deuteron. As a result the high momentum component of the deuteron wave function is not rich enough to dominate in the amplitude of the process $pd \to dp$. On the contrary, mechanisms resulting in excitation of nucleons inside the deuteron due to interaction with an incident beam give a significant contribution to the cross section of the $pd \to dp$ process [1]-[4]. The ^3He nucleus as a more compressed system differs essentially from the deuteron and consequently one can obtain interesting results from investigation of the $p\,^3He \to\ ^3Hep$ process.

The cross section of backward elastic $p\,^3He$-scattering at the kinetic energy of incident proton $T_p > 1$ GeV displays three remarkable peculiarities [7, 8]. (i) In the Born approximation only one mechanism of the process $p^3He \to\ ^3Hep$ dominates, it is the so-called sequential transfer (ST) of the noninteracting np-pair (Fig.1). The contribution from the mechanisms of nonsequential transfer (NST), interacting np-pair transfer (IPT) and deuteron exchange is negligible. In Refs. [9] -[11] the heavy particle stripping (*et id.* two-nucleon transfer) was also investigated and found to be important at back angles for $T_p \leq 0.6$ GeV. However the phenomenological ^3He wave functions restricted to the two-body configuration, which does not permit ST-mechanism were used in that analysis. The other group of papers [12, 13] based on the microscopic optical potential constructed using antisymmetrized pN-amplitudes gives a qualitative explanation of a rise of the cross section at backward angles at energies $T_p \leq 0.6$ GeV without taking into account the heavy particle stripping mechanism. An application of that method at higher energies $T_p > 1$GeV is very complicated due to lack of the experimental information about the elastic formfactor of ^3He in the relevant region of the Δ variable. (ii) The channel $\nu = 1$ (in the notation of Ref.[14]) of the Faddeev component $\varphi^{23}(\mathbf{q}_{23}, \mathbf{p}_1)$ of the ^3He wave function plays the most important role in the np-pair transfer mechanism. This channel corresponds to the orbital momentum $L = 0$, spin $S = 0$, isotopic spin $T = 1$ of two nucleons with numbers 2 and 3 and the orbital momentum $l = 0$ of the nucleon spectator denoted by the number 1. If this channel is excluded from the full wave function $\Psi = \varphi^{23} + \varphi^{31} + \varphi^{12}$, the cross section falls by several orders of magnitude. (iii) Rescatterings in the initial and final states decrease the cross section at $\theta_{c.m.} = 180^0$ considerably in comparison with the Born approximation and make it agree satisfactorily with the available experimental data [15] for $T_p > 0.9$ GeV.

Owing to this evident connection between the structure of ^3He nucleus and the

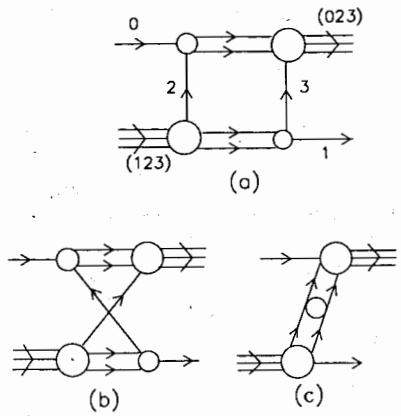

Figure 1: The np-pair transfer mechanisms of the backward elastic $p\,{}^3He$-scattering denoted as $0 + (123) \to 1 + (023)$: a – sequential transfer (ST), b – nonsequential transfer (NST), c – interacting pair transfer (IPT).

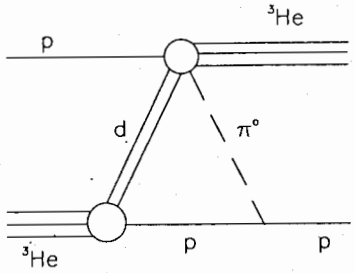

Figure 2: The triangular diagram of one-pion exchange (OPE) with the subprocess $pd \to {}^3He\pi^o$ for backward elastic $p\,{}^3He$ scattering.

dominating mechanism one can hope to obtain an information about high momentum components of the ${}^3He$ wave function from the cross section of the $p{}^3He \to {}^3Hep$ process. However, in Refs. [7, 8] it was mentioned that the D-components of ${}^3He$ wave function are of surprisingly minor importance in the process under discussion at $T_p > 1$ GeV. Moreover, relativistic effects estimated in Ref. [8] at $T_p \sim 1$ GeV by means of substituting the relativistic arguments into the ${}^3He$ wave function instead of the nonrelativistic ones give rather small contribution to the cross section. For this reason, in Refs. [7, 8] it was concluded that the sensitivity of the $p\,{}^3He \to {}^3Hep$ cross section to the high momentum components of the ${}^3He$ wave function is rather weak in spite of high momenta transferred at $T_p > 1$ GeV. Moreover, as was found in [15], the role of the triangular diagram of one-pion exchange (OPE) with the subprocess $pd \to {}^3He\pi^o$ related to the Δ - and double Δ-excitation is in qualitative agreement with the absolute value of the experimental cross section at $T_p > 0.5$ GeV.

In the present work it is shown that the absolute value of the $p\,{}^3He \to {}^3Hep$ cross section at $\theta_{c.m.} = 180^o$ and $T_p > 1$ GeV is determined mainly by the high momentum component of the Faddeev S-wave function of ${}^3He$, $\varphi^{23}(\mathbf{q}_{23}, \mathbf{p}_1)$, associated with the relative momentum $\mathbf{q}_{23}$. On the other hand, rather low values of the "spectator" momentum $\mathbf{p}_1$ are involved in the amplitude of this process. The cross section is calculated also in framework of the OPE mechanism. The relative contribution of the OPE mechanism to the cross section is found to be small in comparison with the np-pair transfer mechanism. We show that this result is directly connected to the high momentum component presented in the ${}^3He$ wave function. It is shown also that due to rescatterings in the initial and final states the cross section calculated with the OPE mechanism is an order of magnitude lower in comparison with the experimental data.

The paper is organized in the following way. Some elements of the formalism for the np-pair transfer mechanism and the OPE amplitude are presented in the next section. The formulas for the ${}^3He$ charge formfactor are also derived there for the channel $\nu = 1$ of the three-body wave function of ${}^3He$ and for the $d + p$ configuration. Numerical results and discussions are given in the section 3. The detail formulas for the np-transfer mechanism in the S-wave approximation are presented in the Appendix with the analytical gaussian parametrization of the wave function and the corresponding numerical parameters are given there.

2 Formalism

2.1 np-pair transfer mechanism

The total formalism for the np-pair transfer mechanism of the backward elastic $p\,{}^3He$-scattering was developed in detail in Refs. [7, 8]. We use here this formalism in the particular case of the S-wave component of the ${}^3He$ wave function.

In the Born approximation the amplitude of transfer of two nucleons with numbers 2 and 3 in the process $0 + \{123\} \to 1 + \{023\}$ (et id. $p\,{}^3He \to {}^3Hep$) can be written

as [7, 8]

$$T_B = 6(2\pi)^{-3}\int d^3q_{23}L_{23}(q_{23},p_1)\chi^+_{p'}(1)\{\varphi_f^{23+}(0;23)\varphi_i^{31}(2;31)+$$
$$\varphi_f^{02+}(3;02)\varphi_i^{31}(2;31)+\varphi_f^{30+}(2;30)\varphi_i^{31}(2;31)\}\chi_p(0), \quad (1)$$

where $\varphi^{ij}(k;ij)=\varphi^{ij}(\mathbf{q}_{ij},\mathbf{p}_k)$ is the Faddeev component of the wave function of the bound state $\{ijk\}$, $\chi_p(\chi_{p'})$ is the spin – isotopic spin wave function of the incident (final) proton; $L_{23}=\varepsilon+\mathbf{q}_{23}^2/m_p+3\mathbf{p}_1^2/4m_p$, m_p is the proton mass, ε is the ^3He binding energy. The subscripts i and f in Eq.(1) refer to the initial and final nucleus respectively. The terms $\varphi_f^{23+}\varphi_i^{31}$, $\varphi_f^{02+}\varphi_i^{31}$, $\varphi_f^{30+}\varphi_i^{31}$ correspond to the IPT, ST and NST mechanisms respectively. In the explicit form the ST mechanism has the following structure of the arguments of the wave functions

$$\varphi_f^{02+}\varphi_i^{31}=\varphi_f^{02+}(\mathbf{q}_{02}=-\frac{1}{2}\mathbf{q}_{23}-\frac{3}{4}\mathbf{Q}_0,\mathbf{p}_3=\mathbf{q}_{23}-\frac{1}{2}\mathbf{Q}_0)$$
$$\times\varphi_i^{31}(\mathbf{q}_{31}=-\frac{1}{2}\mathbf{q}_{23}+\frac{3}{4}\mathbf{Q}_1,\mathbf{p}_2=-\mathbf{q}_{23}-\frac{1}{2}\mathbf{Q}_1), \quad (2)$$

where $\mathbf{Q}_0(\mathbf{Q}_1)$ is the momentum of incident (final) proton in the c.m.s of the final (initial) ^3He nucleus. As was noted in [8], at the scattering angle $\theta_{c.m.}=180°$ two of four momenta in Eq.(2) can simultaneously become equal to zero at integration over $\mathbf{q}_{23}$. On the contrary, in the corresponding formulas for the IPT and NST mechanisms only one argument can be equal to zero while the other three have large values $\sim|\mathbf{Q}_1|=|\mathbf{Q}_0|$ (see Appendix). This makes the ST term dominate in Eq.(1). Indeed, the ST mechanism takes place only if the channels with the isotopic spin $T=1$ of the pair of nucleons {ij} are included into the component $\varphi^{ij}(ij;k)$ either in the initial or final state. It is the direct consequence of the fact that the ST diagram in Fig.1, *a* either starts with or ends in the pp-interaction. The ^3He wave function from Ref. [14] contains only one such channel ($\nu=1$), namely, with the $^1S_0$ state of the NN-pair. In the S-wave approximation for the ^3He wave function the cross section decreases by 5-6 orders of magnitude for $T_p>1$ GeV if the channel $\nu=1$ is excluded [16]. The channels with $\nu\neq1$ corresponding to the isotopic spin $T=0$ of the NN-pair (in particularly, the D-components) can enter the ST-amplitude only in combination with the channel $\nu=1$. For this reason the role of those channels is not so significant.

Since the contribution of the interacting pair transfer mechanism is insignificant [8] we will discuss here only the amplitude of noniteracting pair transfer (NPT) which is the sum of ST and NST amplitudes, IPT=ST+NST. On the basis of the formalism [8] the spin structure of the NPT amplitude in the S-wave approximation for the ^3He wave function can be written in the following form

$$T_B^{\sigma'm'\sigma m}(NPT)=-6(2\pi)^{-3}\sum_{\nu,\nu'=1,2}\int d^3q_{23}L_{23}(\mathbf{q}_{23},\mathbf{p}_1)$$
$$\times\Phi_{\nu'}(q_{02},p'_3)\left[\Phi_\nu(q_{12},p_3)\,a_{S'S}^{\sigma'm'\sigma m}-\Phi_\nu(q_{31},p_2)\,b_{S'S}^{\sigma'm'\sigma m}\right], \quad (3)$$

where $S(S')=0$ for $\nu(\nu')=1$ and $S(S')=1$ for $\nu(\nu')=2$; $\sigma(\sigma')$ and $m(m')$ are the spin z-projections of the initial (final) proton and the ^3He nucleus, respectively;

$$a_{S'S}^{\sigma'm'\sigma m}=\left(f_{S'S0}^{\sigma'm'\sigma m}+f_{S'S1}^{\sigma'm'\sigma m}\right)(A_{T'0}A_{T0}+A_{T'1}A_{T1}),$$
$$b_{S'S}^{\sigma'm'\sigma m}=\left(f_{S'S0}^{\sigma'm'\sigma m}+f_{S'S1}^{\sigma'm'\sigma m}\right)(A_{T'0}A_{T0}-A_{T'1}A_{T1}), \quad (4)$$

here

$$f_{S'S\tilde{S}}^{\sigma'm'\sigma m}=(2\tilde{S}+1)3\sum_M(\tilde{S}M\tfrac{1}{2}\sigma|\tfrac{1}{2}m')(\tilde{S}M\tfrac{1}{2}\sigma'|\tfrac{1}{2}m)A_{S'\tilde{S}}A_{S\tilde{S}}, \quad (5)$$

$$A_{S'S}=\sum_{j=0,1}(-1)^j(2j+1)W(\tfrac{1}{2}\tfrac{1}{2}\tfrac{1}{2}\tfrac{1}{2};Sj)W(\tfrac{1}{2}\tfrac{1}{2}\tfrac{1}{2}\tfrac{1}{2};S'j), \quad (6)$$

$A_{T'T}$ is defined similarly to $A_{S'S}$. The Jacobi relative momenta can be written as

$$\mathbf{q}_{02}=-\frac{1}{2}\mathbf{q}_{23}-\frac{3}{4}\mathbf{Q}_0,\quad \mathbf{p}'_3=\mathbf{q}_{23}-\frac{1}{2}\mathbf{Q}_0,$$
$$\mathbf{q}_{31}=-\frac{1}{2}\mathbf{q}_{23}+\frac{3}{4}\mathbf{Q}_1,\quad \mathbf{p}_2=-\mathbf{q}_{23}-\frac{1}{2}\mathbf{Q}_1,$$
$$\mathbf{q}_{12}=-\frac{1}{2}\mathbf{q}_{23}-\frac{3}{4}\mathbf{Q}_1,\quad \mathbf{p}_3=\mathbf{q}_{23}-\frac{1}{2}\mathbf{Q}_1. \quad (7)$$

In the nonrelativistic case the momenta $\mathbf{Q}_1$ and $\mathbf{Q}_0$ are expressed by the momenta of the observed particles as

$$\mathbf{Q}_1=\frac{1}{3}\mathbf{p}'_h-\mathbf{p},\quad \mathbf{Q}_0=\frac{1}{3}\mathbf{p}_h-\mathbf{p}', \quad (8)$$

where $\mathbf{p}_h(\mathbf{p}'_h)$ is the momentum of the initial (final) ^3He nucleus and $\mathbf{p}(\mathbf{p}')$ is the momentum of the initial (final) proton in the $p+{}^3He$ c.m.s.

Performing summation over the channels $\nu,\nu'=1,2$ one obtains

$$T_B^{\sigma'm'\sigma m}(NPT)=-6(2\pi)^{-3}\Big\{M_0\delta_{\sigma m'}\delta_{\sigma' m}+\sum_\lambda(1\lambda\tfrac{1}{2}\sigma|\tfrac{1}{2}m')$$
$$\times(1\lambda\tfrac{1}{2}\sigma'|\tfrac{1}{2}m)M_1\Big\}, \quad (9)$$

$$M_0=\frac{1}{24}\left(5I_{33}^{11}-4I_{32}^{11}\right)+\frac{3}{8}I_{33}^{22}+\frac{1}{8}\left(I_{33}^{12}-2I_{32}^{12}\right)+\frac{1}{8}\left(I_{33}^{21}-2I_{32}^{21}\right), \quad (10)$$

$$M_1=\frac{1}{8}\left(5I_{33}^{11}+4I_{32}^{11}\right)+\frac{1}{8}I_{33}^{22}-\frac{1}{8}\left(I_{33}^{12}+2I_{32}^{12}\right)-\frac{1}{8}\left(I_{33}^{21}+2I_{32}^{21}\right), \quad (11)$$

$$I_{kl}^{\nu'\nu}\equiv I_{(0i)k;(j1)l}^{\nu'\nu}=\frac{1}{(4\pi)^2}n_{\nu'}n_\nu\int d^3q_{23}L(\mathbf{q}_{23},\mathbf{p}_1)\Phi_{\nu'}(q_{0i},p_k)\Phi_\nu(q_{j1},p_l). \quad (12)$$

The integral $I_{33}^{\nu'\nu}$ corresponds to the NST-mechanism whereas $I_{32}^{\nu'\nu}$ describes the ST mechanism. The amplitude T_B in Eq. (1) is related to the invariant amplitude A by the following formula

$$A_B = 4m_p m_h T_B, \tag{13}$$

the connection of this amplitude with the cross section is given in the next section by Eq.(19). The total wave function of the ^3He nucleus $\Psi = \varphi^{12} + \varphi^{23} + \varphi^{31}$ in Eq. (1) is normalized as

$$\int |\Psi(\mathbf{q},\mathbf{p})|^2 \frac{d^3q\, d^3p}{(2\pi)^6} = 1. \tag{14}$$

2.2 Spin-spin correlation parameter

The spin-spin correlation parameter Σ is calculated here as an additional test of the np-transfer mechanism of the process $\vec{p}\,^3\vec{H}e \to {}^3Hep$ with polarized beam and target. This parameter is defined as

$$\Sigma = \frac{d\sigma(\uparrow\uparrow) - d\sigma(\uparrow\downarrow)}{d\sigma(\uparrow\uparrow) + d\sigma(\uparrow\downarrow)}, \tag{15}$$

where $d\sigma(\uparrow\uparrow)/d\Omega$ and $d\sigma(\uparrow\downarrow)/d\Omega$ are the cross sections for parallel and antiparallel spins of colliding particles, respectively. From Eq. (9) follows that the sum of ST and NST amplitudes in the S-wave approximation is not zero only for $m' + \sigma' = m + \sigma$. Consequently from 16 amplitudes given by Eq.(3) the nonvanishing ones are the following

$$\begin{aligned} T_1 \equiv T^{++++} = T^{----} &= M_0 + \frac{1}{3}M_1, \\ T_2 \equiv T^{+-+-} = T^{-+-+} &= \frac{2}{3}M_1, \\ T_3 \equiv T^{-++-} = T^{+--+} &= M_0 - \frac{1}{3}M_1. \end{aligned} \tag{16}$$

From Eqs. (15) and (16) one finds

$$\Sigma = \frac{|T_1|^2 - |T_2|^2 - |T_3|^2}{|T_1|^2 + |T_2|^2 + |T_3|^2} = \frac{2}{3}\frac{Re(M_1 M_0^*) - \frac{1}{3}|M_1|^2}{|M_0|^2 + \frac{1}{3}|M_1|^2}. \tag{17}$$

2.3 The OPE mechanism

An obvious modification of the formalism of the triangular OPE diagram from Ref. [4] is used here for the OPE amplitude. According to common rules of the diagram technique the amplitude corresponding to the triangular diagram in Fig. 2 takes the following form

$$\begin{aligned} A_{OPE}^{\sigma'm'\sigma m}(ph \to ph) = \int \frac{d^3p_d dT_d}{(2\pi)^4} \sum_{\lambda_d \sigma_p} A_{\sigma\lambda_d}^{m'}(pd \to {}^3He\pi^0) \\ \times \frac{G_m^{\lambda_d\sigma_p}({}^3He \to d+p) < \pi^0 p|p' >}{(k^2 - \mu^2 + i\epsilon)(2m_p T_p - \mathbf{p}_p^2 + i\epsilon)(2m_d T_d - \mathbf{p}_d^2 + i\epsilon)}, \end{aligned} \tag{18}$$

where $\mathbf{p}_i$ is the momentum, T_i is the kinetic energy and m_i is the mass of the i-th intermediate particle (proton or deuteron); k and μ are the 4-momentum and mass of the virtual π- meson, respectively. In Eq.(18) the summation refers to the spin states of the intermediate deuteron (λ_d) and proton (σ_p). The invariant amplitude A of the process $ab \to cd$ in Eq. (18) is related to the corresponding differential cross section in the c.m.s. by the following formula

$$\frac{d\sigma}{d\Omega} = \frac{1}{64\pi^2 s_{ab}} \frac{q_{cd}}{q_{ab}} \overline{|A|^2}, \tag{19}$$

where s_{ab} is the square of the invariant mass of the system $a+b$, q_{ij} is the relative momentum in the system $i+j$. The amplitude of the virtual decay $^3He \to d+p$ has the form

$$G_m^{\lambda_d\sigma_p}({}^3He \to d+p) = \sqrt{S_{pd}^h}\, 4m_p\sqrt{m_h}(\varepsilon_h + \frac{2}{3}\frac{\mathbf{Q}^2}{m_p})\psi_m^{\lambda_d\sigma_p}(\mathbf{Q}); \tag{20}$$

here m_h is the mass of the ^3He nucleus, $S_{pd}^h \simeq 1.5$ is the spectroscopic factor of ^3He in the channel $d+p$ [20]; $\psi_m^{\lambda_d\sigma_p}(\mathbf{Q}) = < {}^3He|d,p >$ is the overlap integral between the ^3He wave function Ψ_m and the production of the wave functions of deuteron ψ_{λ_d} and proton φ_{σ_p}. This wave function is normalized by the following condition

$$\frac{1}{2J_h+1} \sum_{m,\lambda_d,\sigma_p} \int |\psi_m^{\lambda_d\sigma_p}(\mathbf{Q})|^2 \frac{d^3Q}{(2\pi)^3} = 1. \tag{21}$$

The Fourier-transformation of this function is given by

$$\psi_m^{\lambda_d\sigma_p}(\mathbf{Q}) = \int \exp(-i\mathbf{Q}\mathbf{r})\psi_m^{\lambda_d\sigma_p}(\mathbf{r}) d^3r, \tag{22}$$

where the wave function in the coordinate space has the following form

$$\begin{aligned} \psi_m^{\lambda_d\sigma_p}(\mathbf{r}) = < \varphi_{\sigma_p}\, \psi_{\lambda_d}(\boldsymbol{\rho})|\Psi_m(\boldsymbol{\rho},\mathbf{r}) > = \\ = \sum_{L,M,S,M_S} (L\,M\,S\,M_S|\frac{1}{2}m)(1\lambda_d\frac{1}{2}\sigma_p|SM_S)\, U_L(r)\, Y_{LM}(\hat{\mathbf{r}}); \end{aligned} \tag{23}$$

here $S = 3/2$ for $L = 2$ and $S = 1/2$ for $L = 0$. The spherical functions Y_{LM} and Clebsh-Gordan coefficients are used in Eq.(23) in the standard notations. The $S-$ and $D-$components of the wave function $U_L(r)$ in Eq. (23) were obtained in Ref.[21] by numerical solution of the Faddeev equations with the NN-interaction in the form of Reid soft core (RSC). The results [21] are used here with the following normalization condition

$$\int_0^\infty \left[U_0^2(r) + U_2^2(r)\right] r^2 dr = 1. \tag{24}$$

Actually the three-body calculations for the normalization integral (24) give the value 0.43 [22]. Consequently the contribution of the OPE diagram in Fig. 2 is overestimated by the condition given in Eq.(24). However there are no experimental data at present

about the differential cross section of the reaction $pd^* \to {}^3He\pi^0$, where d^* is the singlet deuteron.. Under assumption that the cross sections of the reactions $pd \to {}^3He\pi^0$ and $pd^* \to {}^3He\pi^0$ are equal to each other, the normalization condition in Eq. (24) effectively takes into account the contribution of the $p + d^*$ configuration with pn-pair in the singlet state.

The vertex function πNN has the following form [23] ,

$$< \pi^0 p|p' >= 2m_p \frac{f_{\pi NN}}{\mu} \varphi^+_{\sigma'}(\boldsymbol{\sigma}\mathbf{Q})\varphi_{\sigma_p} F_{\pi NN}(k^2), \tag{25}$$

here φ_{σ_p} and $\varphi_{\sigma'}$ are the Pauli spinors for nucleons, $f_{\pi NN} = 1$;

$$\mathbf{Q} = \sqrt{\frac{E_p + m_p}{E_{p'} + m_p}}\mathbf{p}_{p'} - \sqrt{\frac{E_{p'} + m_p}{E_p + m_p}}\mathbf{p}_p, \tag{26}$$

E_p, $(E_{p'})$ is the total energy of the proton $p(p')$;

$$F_{\pi NN}(k^2) = \frac{\Lambda_\pi^2 - \mu^2}{\Lambda_\pi^2 - k^2}. \tag{27}$$

For the cutoff parameter Λ_π in the monopole πNN formfactor defined by Eq.(27) the value $\Lambda_\pi = 0.65$ GeV/c is used here [24, 23].

As is shown numerically in the next section, the contribution of the D-component to the OPE cross section is negligible. In the S-wave approximation for the ${}^3He \to d + p$ channel the cross section of the $p^3He \to^3 Hep$ process can be expressed through the cross section of the reaction $pd \to {}^3He\pi^0$ in the following way

$$\frac{d\sigma}{d\Omega_{c.m.}} = \frac{1}{64\pi^2}\frac{1}{s_{ph}}\overline{|A^{\sigma' m' \sigma m}_{OPE}|} =$$

$$= \frac{m_p\, m_h}{2\pi}\frac{E_{p'} + m_p}{E^2_{p'}}\left(\frac{f_{\pi NN}}{\mu}\right)^2 S^h_{pd} F^2_{\pi NN}(k^2)\frac{s_{pd}}{s_{ph}}\frac{q_{pd}}{q_{\pi h}}\frac{d\sigma}{d\Omega_{c.m.}}(pd \to {}^3He\pi^o)$$

$$\times \left|i\kappa\mathcal{F}_0(\tilde{p}) + \mathcal{W}_{10}(\tilde{p}, \tilde{\delta})\right|^2, \tag{28}$$

where

$$\mathcal{F}_l(\tilde{p}) = \int_0^\infty U_l(r)\, j_l(\tilde{p}r)\, r dr,$$

$$\mathcal{W}_{lL}((\tilde{p}, \tilde{\delta}) = \int_0^\infty j_l(\tilde{p}r) U_L(r)(i\tilde{\delta} + 1)\exp(-i\tilde{\delta}r) dr. \tag{29}$$

$$\kappa = 2m\left(\frac{1}{E_{p'} + m} + \frac{1}{E_{p'}}\right)|\mathbf{p}_{p'}|, \quad \tilde{\mathbf{p}} = \frac{2m}{E_{p'}}\mathbf{p}_{p'}, \tag{30}$$

$$\tilde{\delta}^2 = \tilde{\mathbf{p}}^2 + (2mT_{p'} + \mu^2 - 2\varepsilon_h m_p)\frac{2m_p}{E_{p'}}, \tag{31}$$

$$k^2 - \mu^2 = \frac{E_{p'}}{2m_p}\left(\tilde{\mathbf{p}}^2 - \tilde{\delta}^2\right); \tag{32}$$

in Eqs.(28-32) $E_{p'} = \sqrt{m_p^2 + \mathbf{p}^2_{p'}}$ is the total energy, $\mathbf{p}_{p'}$ is the momentum and $T_{p'}$ is the kinetic energy of the secondary proton in the laboratory system.

Rescatterings in the initial and final states for the OPE mechanism are taken into account here in the line of work [8] on the basis of Glauber-Sitenko theory. According to Ref. [8], the amplitude A^{dist}_{fi} for the exchange mechanism with rescatterings in the $p\ {}^3He \to {}^3Hep$ process can be related to corresponding amplitude in the Born approximation A_B by the following expression

$$A^{dist}_{fi} = A_B(\mathbf{p}'_h, \mathbf{p}'; \mathbf{p}_h, \mathbf{p}) + \frac{i}{4\pi p}\int d^2q\, F_{ph}(\mathbf{q}) A_B(\mathbf{p}'_h, \mathbf{p}'; \mathbf{p}_h + \mathbf{q}, \mathbf{p} - \mathbf{q})$$

$$+\frac{i}{4\pi p'}\int d^2q'\, f_{pp}(\mathbf{q}') A_B(\mathbf{p}'_h - \mathbf{q}', \mathbf{p}' + \mathbf{q}'; \mathbf{p}_h, \mathbf{p})$$

$$-\frac{1}{(4\pi)^2 p'p}\int\int d^2q d^2q'\, F_{ph}(\mathbf{q}) f_{pp}(\mathbf{q}') A_B(\mathbf{p}_h - \mathbf{q}', \mathbf{p}' + \mathbf{q}'; \mathbf{p}_h + \mathbf{q}, \mathbf{p} - \mathbf{q}). \tag{33}$$

In Eq. (33) the amplitudes f_{pp} and F_{ph} describe the elastic $pp-$ and $p\ {}^3He-$ forward scattering, respectively. The last three terms in Eq. (33) take into account rescatterings in the intial, final state and simultaneously in the initial and final states, respectively. In the spinless approximation the amplitude of pN-scattering is parametrized in the standard form [25]

$$f_{pN}(q) \equiv k_{pN} A_{pN}\exp(-B_{pN}q^2) = \frac{k_{pN}\sigma_N}{4\pi}(i + \alpha_N)\exp(-\frac{1}{2}\beta_N q^2), \tag{34}$$

where q is the momentum transferred in pN-scattering, k_{pN} is the wave vector of the nucleon in the $p + N$ c. m. s., σ_N is the total cross section of the pN-scattering, α_N and β_N are the phenomenological parameters fitted to the experimental data on pN-scattering [26]. Using the gaussian form for the ${}^3He$ density and Eq. (34) one gets an analytical form for the amplitude F_{ph}

$$F_{ph}(q) = k_{ph}\sum_{k=1}^{3} A^{ph}_k \exp(-B^{ph}_k q^2); \tag{35}$$

here k_{ph} is the the wave vector of the nucleon in the $p + {}^3He$ c. m. s.; parameters A^{ph}_k, B^{ph}_k are expressed analytically through parameters of pN-scattering amplitude (34) and the oscillator radius of the gaussian form for the ${}^3He$ nucleus density [27]. Three terms in Eq. (35) correspond to single, double and triple scattering of the incident proton from nucleons of the ${}^3He$ nucleus. Since the OPE amplitude in the Born approximation given by Eq.(18) is a smooth function of the kinematic variables $\mathbf{p}_h$, $\mathbf{p}'_h$, $\mathbf{p}$, $\mathbf{p}'$, one can take this amplitude outside of the sign of integrals over d^2q and d^2q' in Eq. (33) [1]. In this approximation the OPE amplitude with rescatterings has the following form

$$A^{dist}_{OPE} = D\, A^{\sigma' m' \sigma m}_{OPE}, \tag{36}$$

[1]When calculating the contribution of the rescatterings to the np-transfer amplitude the integrations over d^2q and d^2q' in Eq.(33) are performed exactly in analytical form. In this case the factorization like in Eq. (36) does not occure.

where the amplitude $A_{OPE}^{\sigma' m' \sigma m}$ was defined by Eq.(18) and the distortion factor has the form

$$D = 1 + \frac{iA_{pp}}{4\beta_{pp}} + \sum_k \left[\frac{iA_k^{ph}}{4B_k^{ph}} - \frac{A_{pp}A_k^{ph}}{16\beta_{pp}B_k^{ph}} \right]; \qquad (37)$$

parameters A_{pp}, β_{pp}, A_k^{ph}, B_k^{ph} are defined in Eqs. (34,35).

2.4 The charge formfactor of ^3He

In the nonrelativistic impulse approximation the charge formfactor of ^3He is defined as

$$ZF_{ch}(\Delta) = \int\int \exp(i\mathbf{\Delta x})\Psi^+(1,2,3)\hat{\rho}_{ch}(\mathbf{x},\mathbf{r}_i)\Psi(1,2,3)d\mathbf{x}\prod_{i=1}^{3} d\mathbf{r}_i, \qquad (38)$$

where $Z = 2$ and the charge density operator has the following form

$$\hat{\rho}_{ch}(\mathbf{x},\mathbf{r}_i) = \sum_{i=1}^{3}\left\{\frac{1}{2}[1+\tau_z(i)]f_{ch}^p(\mathbf{x}-\mathbf{r}_i) + \frac{1}{2}[1-\tau_z(i)]f_{ch}^n(\mathbf{x}-\mathbf{r}_i)\right\}; \qquad (39)$$

here τ_z is the Pauli matrix for the z-projection of the nucleon isotopic spin, $\mathbf{r}_i$ is the coordinate of the i-th nucleon, $f_{ch}^N(\mathbf{y})$ is the distribution of the nucleon charge density, which is related to the charge formfactor of the nucleon in the following way

$$F_{ch}^N(\mathbf{q}) = \int \exp(i\mathbf{yq}) f_{ch}^N(\mathbf{y})d\mathbf{y}; \qquad (40)$$

$\Psi(1,2,3) = \varphi^{23} + \varphi^{12} + \varphi^{31}$ is the antisymmetrized wave function of ^3He nucleus, $\mathbf{\Delta} = \mathbf{p}_h' - \mathbf{p}_h$ is the transferred momentum. As was mentioned above, in the backward elastic $p\,^3He$-scattering the main contribution gives the channel $\nu = 1$ of the Faddeev wave function φ^{23}. The following expression can be obtained for the charge formfactor of the ^3He nucleus taking into account only one channel $\nu = 1$ in the ^3He wave function

$$F_{ch}(\Delta) = 3(F^p + \frac{1}{2}F^n)J^{23;23}(\Delta) + (\frac{1}{4}F^p + \frac{1}{2}F^n)J^{23;31}(\Delta); \qquad (41)$$

here the integrals $J^{23;31}$ and $J^{23;23}$ are defined by the following formulas

$$J^{23;23}(\Delta) = \frac{1}{(4\pi)^2}\int\int d\mathbf{q}d\mathbf{p}\Phi_{\nu'}(|\mathbf{q}|,|\mathbf{p}-\frac{2}{3}\mathbf{\Delta}|)\Phi_{\nu}(|\mathbf{q}|,|\mathbf{p}|);$$

$$J^{23;31}(\Delta) = \frac{1}{(4\pi)^2}\int\int d\mathbf{q}d\mathbf{p}\Phi_{\nu'}(|\mathbf{q}|,|\mathbf{p}-\frac{2}{3}\mathbf{\Delta}|)$$

$$\times\Phi_{\nu}(|-\frac{1}{2}\mathbf{q}+\frac{3}{4}\mathbf{p}|,|-\mathbf{q}-\frac{1}{2}\mathbf{p}|). \qquad (42)$$

In the framework of the $d+p$-configuration for the ^3He nucleus given by Eqs. (23) and (24) we obtain the following expression for the ^3He charge formfactor:

$$F_{ch}(\Delta) = \frac{1}{2}F_{ch}^p(\Delta)\left\{F_{000}\left(\frac{2}{3}\Delta\right) + F_{022}\left(\frac{2}{3}\Delta\right)\right\} +$$

$$+\frac{1}{2}[F_{ch}^p(\Delta)+F_{ch}^n(\Delta)]\left\{S_s^d\left(\frac{1}{2}\Delta\right)\left[F_{000}\left(\frac{1}{3}\Delta\right)+\right.\right.$$

$$\left.\left.+F_{022}\left(\frac{1}{3}\Delta\right)\right] + \frac{1}{\sqrt{8\pi}}S_Q^d\left(\frac{1}{2}\Delta\right)\left[\sqrt{8}F_{220}\left(\frac{1}{3}\Delta\right) - F_{222}\left(\frac{1}{3}\Delta\right)\right]\right\}, \qquad (43)$$

where

$$F_{iLL'}(\Delta) = \int_0^\infty j_i(\Delta\rho)U_L(\rho)\,U_{L'}(\rho)\,\rho^2\,d\rho. \qquad (44)$$

Here $S_s^d(\Delta)$, $S_Q^d(\Delta)$ are the scalar and quadrupole formfactors of the deuteron (see, for example, Ref. [17]). The parametrization from Ref. [18] is used here for the nucleon formfactor $F_{ch}^N(\Delta)$.

3 Numerical results and discussions

Numerical calculations for the np-pair transfer mechanism are performed here using the ^3He wave function obtained in Ref.[14] from the solution of Faddeev equations in momentum space with the RSC potential of the NN-interaction in the $^1S_0$ and $^3S_1 - {}^3D_1$-states. The separable analytical parametrization from Ref.[28] is used here for the spatial part Φ_ν of the Faddeev component of the ^3He wave function in Eqs.(3),(12), (42). In the notations of Ref. [28] it has a form

$$\Phi_\nu(q_{23},p_1) = n_\nu\varphi_\nu(q_{23})\chi_\nu(p_1), \qquad (45)$$

where n_ν is the numerical constant [28]. The functions $\varphi(q)$ and $\chi(p)$ in Eq.(45) are normalized according to the following conditions

$$\int_0^\infty \varphi^2(q)q^2dq = 1, \int_0^\infty \chi^2(p)p^2dp = 1. \qquad (46)$$

The square of the functions $\varphi_\nu(q), \chi_\nu(q)$ and the S-component of the deuteron wave function, $u(q)$, for the RSC potential [29] are shown in Fig.3. The results of calculation of the differential cross section are shown in Figs.4-9 in comparison with the experimental data [15].

The numerical results demonstrate the following important features of the process in question. First, the ST-mechanism involves the high momentum components of the S-wave functions $\varphi_\nu(q_{23})$. The ^3He wave function in the channels $\nu = 1$ and $\nu = 2$ is probed at high momenta $\mathbf{q}_{23} > 0.6GeV$ when the cross section is measured at $T_p > 1$ GeV. To show it, in Fig.3 (a) we present the part of the function $\varphi_\nu(q_{23})$ ($\nu = 1$ and 2), denoted as $\tilde{\varphi}_\nu$, which coincides with $\varphi_\nu(q_{23})$ for $q_{23} > 0.6GeV/c$ and differs considerably from it for smaller momenta $q_{23} < 0.5GeV/c$. In Fig.3 (b) we also show the parts of the functions $\chi_\nu(p_1)$, denoted as $\tilde{\chi}_\nu$, which are very close to the corresponding total functions $\chi_\nu(p_1)$ at small spectator momenta $p_1 \sim 0 \div 0.1$GeV/c and are negligible for $p_1 > 0.2$GeV/c. The cross sections calculated with these functions $\tilde{f}_\nu$ instead of

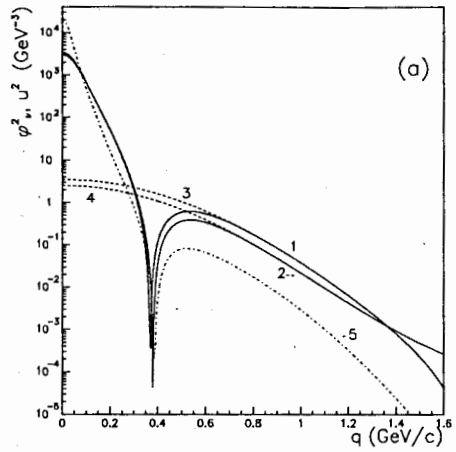

Figure 3: The square of functions $\varphi_\nu(q)$, $\chi_\nu(q)$ from Ref.[28], the S-component of the deuteron wave function $u(q)$ from Ref. [29] and the functions $\widetilde{\varphi}_\nu(q)$ and $\widetilde{\chi}_\nu(q)$ defined in the text. $1 - \varphi_1^2(q)$, $2 - \varphi_2^2(q)$, $3 - \widetilde{\varphi}_1^2(q)$, $4 - \widetilde{\varphi}_2^2(q)$, $5 - u^2(q)$;

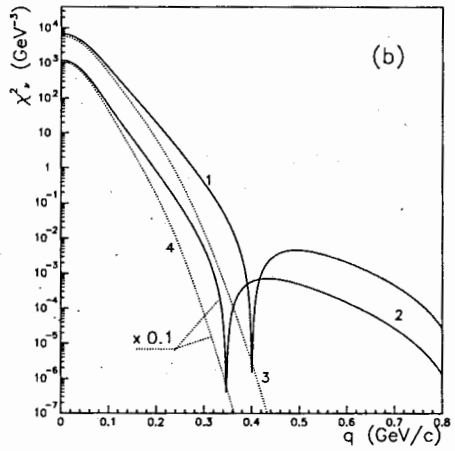

Fig.3, b

The same as in Fig.3,*a* but $1 - \chi_1^2(q)$, $2 - \chi_2^2(q)$, $3 - \widetilde{\chi}_1^2(q)$, $4 - \widetilde{\chi}_2^2(q)$; the curves 2 and 4 in the part *a* are multiplied by factor 10^{-1}.

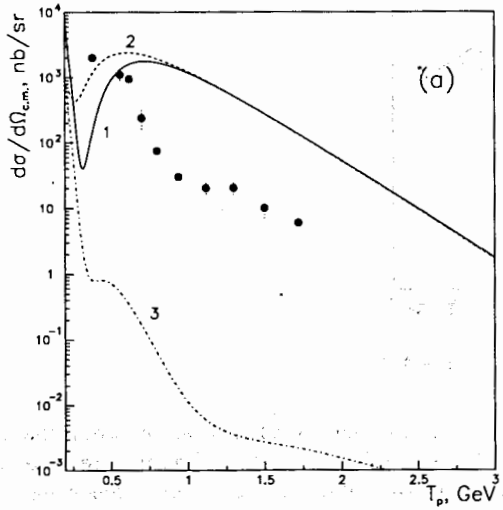

Figure 4: The differential cross section of elastic p^3He scattering at $\theta_{c.m.} = 180^o$ as a function of the incident proton kinetic energy T_p. Curves 1-3 show the results of calculation in the Born approximation for the amplitude in Eq. (1): 1 - with the ^3He wave function from [28], 2 - with $\widetilde{f}_\nu(p_1)$ instead of $f_\nu(p_1)$, 3 - with $\widetilde{f}_\nu(q_{23})$ instead $f_\nu(q_{23})$; *a* - for $f_\nu = \varphi_1$, *b* - for $f_\nu = \chi_1$, *c* - for $f_\nu = \varphi_2$, *d* - for $f_\nu = \chi_2$. The experimental points are taken from Ref.[15]

the full functions f_ν (here $f = \varphi$ or $f = \chi$) are shown in Fig.4 by curves 2. One can see that these curves are very close to the total result obtained with the full functions $\varphi_\nu(q_{23})$ and $\chi_\nu(p_1)$. In contrast, as one can see from Fig.4 (curves 3), the cross section calculated with the complementary parts $\varphi_\nu - \widetilde{\varphi}_\nu$ and $\chi_\nu - \widetilde{\chi}_\nu$ is 5-6 orders of magnitude smaller for $\nu = 1$ and 4-6 times smaller for the channel $\nu = 2$. Obviously the channel $\nu = 1$ of the ^3He wave function plays the most important role in the $p\,^3He \to {}^3Hcp$ process.

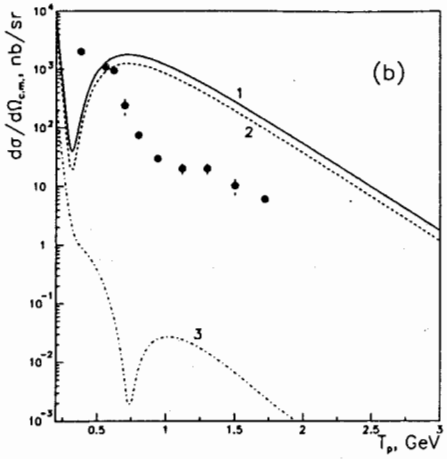

Fig.4, b

Second, the above result demonstrates also that the ST mechanism uses rather low "spectator"-momenta $p_1 \sim 0 \div 0.1 GeV/c$ in the function $\chi_\nu(p_1)$. This feature makes the ST mechanism dominate. The qualitative explanation of these results is following. One can find from Eq.(2), that for $\mathbf{Q}_1 = -\mathbf{Q}_0$ (*et id.* $\theta_{c.m.} = 180°$) the equations $\mathbf{q}_{31} = \mathbf{q}_{02}$ and $\mathbf{p}_2 = -\mathbf{p}_3$ are satisfied. Consequently, the main contribution into the integral over $d\mathbf{q}_{23}$ in Eq. (1) gives the region $|\mathbf{p}_2| = |\mathbf{p}_3| \sim 0$, in which $|\mathbf{q}_{31}| = |\mathbf{q}_{02}| \sim Q_1$. On the contrary, the region of $|\mathbf{q}_{31}| = |\mathbf{q}_{02}| \sim 0$ corresponds to $|\mathbf{p}_2| = |\mathbf{p}_3| \sim 2Q_1$ and plays insignificant role since for $T_p > 1$ GeV the momentum Q_1 is large, $Q_1 > 0.6$ GeV. This question is discussed in detail in the Appendix on the basis of the analytical expression for the np-transfer amplitude in the S-wave approximation.

The contribution of the channel $\nu = 1$ of the wave function to the ^3He charge formfactor, $F_{ch}(\Delta)$, is shown in Fig. 5 by curve 2. Curve 3 in Fig. 5 shows the result for $F_{ch}(\Delta)$ obtained with the function $\tilde{\chi}_1(p_1)$ instead of $\chi_1(p_1)$ and with $\tilde{\varphi}_1(q_{23})$ instead of $\varphi_1(q_{23})$. One can see from this picture that the relative contribution of the channel $\nu = 1$ is maximal at transferred momenta $\Delta > 1.5$ GeV/c, but it is an order of magnitude smaller in comparison with the full result shown by curve 1 in Fig. 5. Moreover, the contribution obtained with the functions $\tilde{\varphi}_1(q_{23})$ and $\tilde{\chi}_1(p_1)$, dominating in the cross section of the backward elastic $p\,^3He$-scattering, is negligible at all transferred momenta. Obviously it is connected to the fact that at high values Δ the charge formfactor $F_{ch}(\Delta)$ involves the high momentum components of the ^3He wave function associated both with the relative momentum q_{23} and the momentum p_1.

Third, we have found numerically that the contribution of the OPE mechanism without taking into account rescatterings is in agreement with the experimental data at $T_p = 0.5 - 1.3$ GeV (curve 4 in Fig.6). However, the ST cross section calculated in

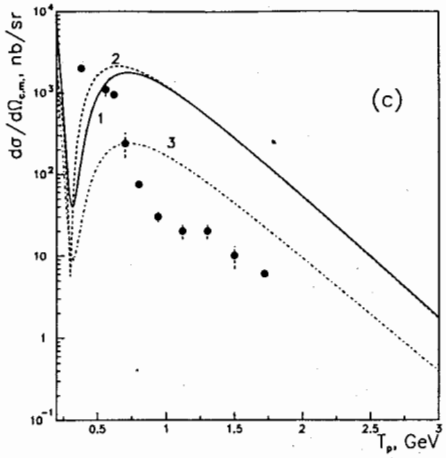

Fig.4, c

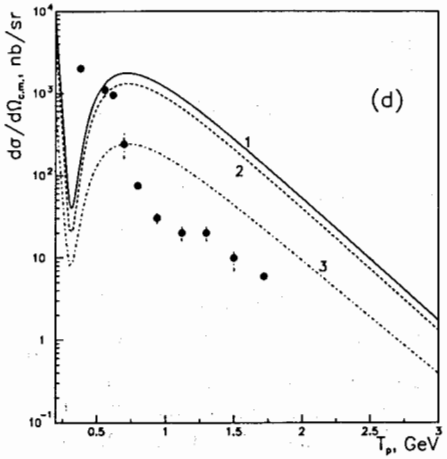

Fig.4, d

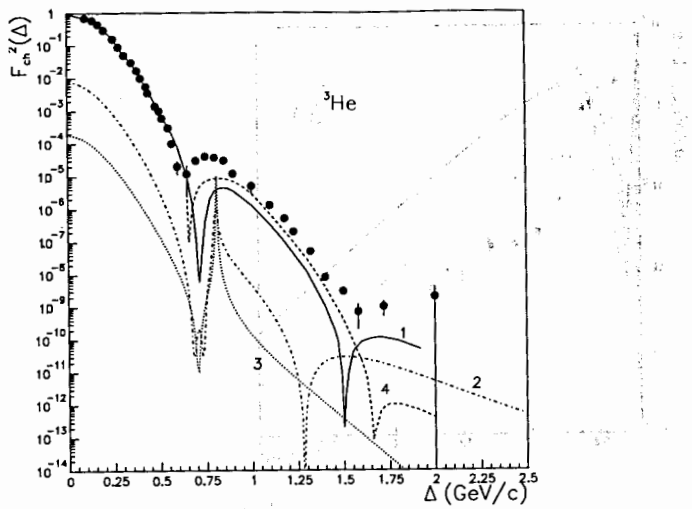

Figure 5: The charge formfactor of the ^3He nucleus calculated in the impulse approximation using dufferent assumptions about the ^3He wave function. Curve 1 – from [28] with the three-body wave function of the ^3He nucleus; curve 2 – with only one channel $\nu = 1$; curve 3 – the same as curve 2 but with $\tilde{\chi}_1(p_1)$ instead of $\chi_1(p_1)$ and $\tilde{\varphi}_1(q_{23})$ instead of $\varphi_1(q_{23})$; curve 4 – with the $d+p$ configuration in Eqs.(23), (24). The circles ($\bullet$) are experimental data from [19].

the Born approximation is by factor $\sim 20-30$ larger than the OPE contribution at $T_p > 0.8$ GeV (curve 1 in Fig.6).

The numerical results show that in the interval of initial energies 0.5- 2.5 GeV the contribution of the D-wave of the $d+p$ channel of the ^3He wave function to the OPE amplitude is very small in comparison with the S-wave contribution. In fact the following numerical relations take place for the formfactors defined by Eq. (29):

$$|\mathcal{F}_2(\tilde{p})| \sim 0.1|\mathcal{F}_0(\tilde{p})|,\ |\mathcal{W}_{12}(\tilde{p},\tilde{\delta})| \sim 0.1|\mathcal{W}_{10}(\tilde{p},\tilde{\delta})|,\ |\mathcal{W}_{32}(\tilde{p},\tilde{\delta})| \sim 0.5|\mathcal{W}_{12}(\tilde{p},\tilde{\delta})|,$$

$$|\mathcal{F}_2(\tilde{p})| \sim |\mathcal{W}_{32}(\tilde{p},\tilde{\delta})|,\ |\mathcal{F}_0(\tilde{p})| \sim 0.3|\mathcal{W}_{10}(\tilde{p},\tilde{\delta})|.$$

The differential cross section of the process $pd \to {}^3He\pi^0$ at the π-meson scattering angle $\theta_{c.m.} = 180^o$ is taken from the experimental data [30]. The wave functions $U_0(r)$ and $U_2(r)$ describing the relative motion in the channel $^3He \to d+p$ according to Eq. (23) are parametrized here in the following form

$$U_0(r) = \sum_{i=1}^{5} S_i \exp(-\kappa_i r^2), \quad U_2(r) = \sum_{i=1}^{5} D_i r^2 \exp(-\lambda_i r^2). \tag{47}$$

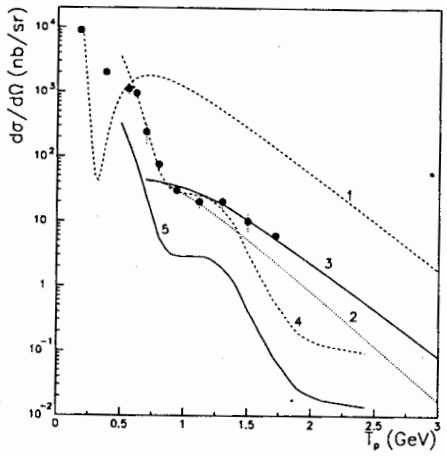

Figure 6: The same as in Fig.4 but curves show the results of calculcalition with OPE and np-pair transfer mechanisms: 1 – Born approximation for the amplitude in Eq. (1) with the ^3He wave function from [28] , 2 – the same as curve 1 but with the deuteron w.f. $u(q_{23})$ instead of $\varphi_1(q_{23})$ and $\varphi_2(q_{23})$; 3 – the same as curve 1 but with allowance for rescatterings in the initial and final states; 4 – OPE in the Born approximation, 5 – OPE with rescatterings.

The numerical coefficients S_i, κ_i, D_i, λ_i are given in Table 1. The $d+p$-configuration of the ^3He nucleus described by Eqs. (23, 24) seems reasonable enough for the evaluation of the OPE amplitude because this configuration approximates the ^3He charge formfactor properly in the wide region of transferred momenta $\Delta = 0 \div 1.5 GeV/c$ (Fig.5).

Taking into account rescatterings in the initial and final states we find that the cross section calculated with OPE mechanism decreases by one order of magnitude and becomes considerably lower than the experimental data (see Fig. 6). The cross section of the $p\,{}^3He \to {}^3Hep$ process for $T_p < 1GeV$ is likely to be defined mainly by the multistep pN-scattering mechanisms discussed in Refs.[12, 13] including the heavy stripping mechanism [9] -[11] also. We stress that the high momentum components of the functions φ_ν in Eq.(45) play the most important role in the competition between the OPE and ST mechanisms. One can see from Fig.3, (a), that the high momentum component of the functions $\varphi_\nu(q)$ is richer in comparison with the deuteron wave function $u(q)$, especially for $q > 0.5$ GeV/c. This is a direct consequence of the fact that the ^3He nucleus is more compact as compared with the deuteron. To compare with the pd-scattering, we performed the calculation of the ST cross section with the S-component of the deuteron wave function $u(q)$ in Eq.(45) instead of the function

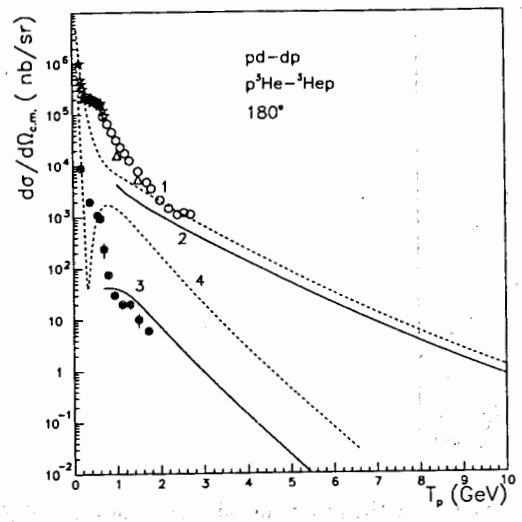

Figure 7: The differential cross sections of backward elastic pd- and $p\,{}^3He$-scattering at $\theta_{c.m.} = 180^o$ versus the kinetic energy of the initial proton T_p. The curves show the results of calculations with the relativistic relative momenta in the vertices $d \to np$ and ${}^3He \to \{23\} + p$: curves 1 and 2 are taken from Ref. [5] for the $pd \to dp$ process in the framework of the nucleon exchange mechanism with RSC wave function of deuteron; 3 and 4 refer to the process $p\,{}^3He \to {}^3Hep$ for np-pair transfer mechanism. Dashed lines (1 and 4) are the Born approximation, full lines (2 and 3) take rescatterings into account. The experimental points are taken from [15] (•), [33] (○), [32] (⋆), [34] (△).

$\varphi_\nu(q_{23})$ for $\nu = 1, 2$. As it seen from curve 2 in Fig. 6, in this case the ST cross section is by a factor ∼40 smaller than with the function $\varphi_\nu(q_{23})$ and close to the OPE cross section in the Born approximation. Note in this connection that in the $pd \to dp$ process the contribution of the neutron exchange mechanism in the Born approximation is not dominating [31] for $T_p > 1$GeV and comparable with the OPE mechanism [4, 5]. This is one of reasons for a very nontrivial problem which arises when one attempts to extract a definite information about the high momentum components of the deuteron wave function from the experimental data on the $pd \to dp$ process.

In Fig.7 the cross sections of the elastic pd- and $p\,{}^3He$-scattering are compared with each other at the angle $\theta_{c.m.} = 180^o$ as a functions of the initial energy T_p. One can see that with increasing initial energy the calculated cross section of the $p\,{}^3He \to {}^3Hep$ process decreases more rapidly than the $pd \to dp$ cross section. The reason for this is the difference between the deuteron and ${}^3He$ masses. Owing to this fact the modulus of momentum $Q_1 = Q_0$ in Eq. (8) for the np-pair transfer mechanism

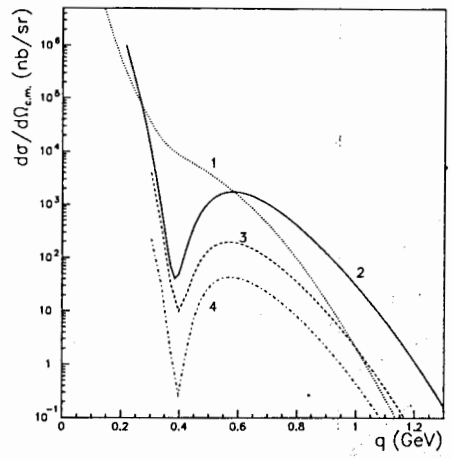

Figure 8: The same as in Fig.7, but versus the relative momentum in the vertices $d \to n + p$ and ${}^3He \to \{23\} + p$. The curves show the results of calculations in the Born approxmation for the neutron exchange in the $pd \to dp$ process (curve 1), and for the np-transfer mechanism of the process $p\,{}^3He \to {}^3Hep$ (curves 2 - 4): 2 – with the ${}^3He$ wave function from Ref. [28], 3 – with the deuteron wave function $u(q)$ instead of $\varphi_1(q)$, 4 – with the deuteron wave function $u(q)$ instead of $\varphi_1(q)$ and $\varphi_2(q)$.

of the $p\,{}^3He \to {}^3Hep$ process increases with growing T_p essentially faster (both in the nonrelativistic and relativistic kinematics) than the relative momentum q_{pn} in the vertex $d \to p + n$ of the pole diagram of the neutron exchange for the $pd \to dp$ process. The results of calculations of these cross sections in the Born approximation are presented in Fig. 8 versus the relative momentum q_{pn} (for the $pd \to dp$ process) and the momentum $Q_1 = Q_0$ (for the $p\,{}^3He \to {}^3Hep$ process).

One can see from this figure that, in contrast to the T_p-dependence, with increasing q the $pd \to dp$ cross section as a function of the internal relative momentum q decreases more rapidly than the $p\,{}^3He \to {}^3Hep$ cross section. These cross sections are equal to each other at the relative momentum ∼ 0.6GeV/c, which corresponds to the kinetic energy $T_p = 2.65$GeV in the $pd \to dp$ process and $T_p = 0.8$GeV in the $p\,{}^3He \to {}^3Hep$ process. With increasing the momenta up to $q \sim 1$GeV/c the cross section of the $pd \to dp$ process becomes an order of magnitude smaller than the $p\,{}^3He \to {}^3Hep$ cross section. At this point the kinetic energy of incident proton equals to 9.3 GeV in $pd-$ and 2.8 GeV in $p\,{}^3He-$ collision. As it seen from Fig.8, after substitution of the deuteron S-wave function $u(q)$ into Eq.(45) instead of the functions φ_1 and φ_2 the cross section of the $pd \to dp$ process decreases still faster than the cross section of the $p\,{}^3He \to {}^3Hep$ process.

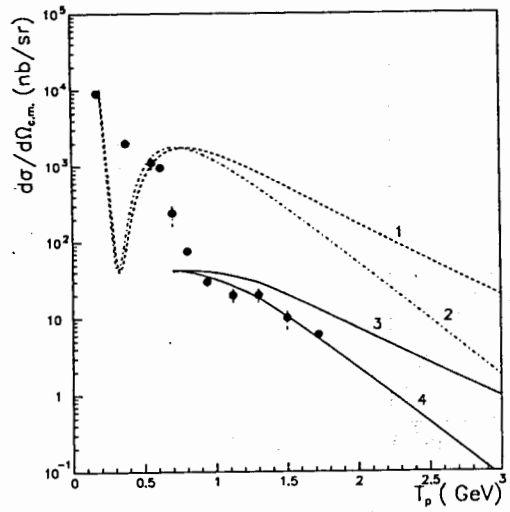

Figure 9: The same as in Figs.4 - 7, but calculated with the relativistic momenta Q_0, Q_1 (curves 1 and 3) according to Ref. [8] and nonrelativisic momenta from Eq. (8) (curves 2 and 4): 1,2 – Born approximation; 3,4 – with rescatterings taken into account.

The above performed comparison shows that an experimental investigation of the backward elastic $p\ ^3He$ scattering at energies of incident protons $T_p \sim 2.5$GeV can give the unique information about the off-energy shell NN-interaction which might be reached in the $pd-$ collision only at more high initial energies ~ 9 GeV.

The role of relativistic effects is estimated here by means of replacement of the non-relativistic momenta $Q_1^{nr} = Q_0^{nr}$ defined in Eqs.(8) with the corresponding relativistic ones $Q_1^{rel} = Q_0^{rel}$ (where $Q^{rel} < Q^{nr}$) defined by Eq. (79) in Ref.[8]. The results of calculations are shown in Fig. 9. As it seen from this figure, a such replacement turns out to be insignificant up to the initial energy $T_p \sim 1$ GeV, in spite of enough large magnitude of the nonrelativistic momentum $Q_0 = Q_1 \sim 0.6$ GeV/c at this energy for the scattering angle $\theta_{c.m.} = 180°$. With increasing the energy above 1 GeV the relativistic result for the cross section becomes considerably higher than the nonrelativistic one, thus at $T_p = 3$ GeV the corresponding difference

is about an order of magnitude. At this energy the nonrelativistic momentum $Q_1 = Q_0$ takes the value ~1.05 GeV/c. The relation between the relativistic and nonrelativistic result is not changed by the rescatterings. Therefore, in complete future analysis of this process one should take into account relativistic effects in a consistent way. Note, that in the present work the agreement with experiment is better for the nonrelativistic calculations than for the relativistic ones. Perhaps, it is connected to

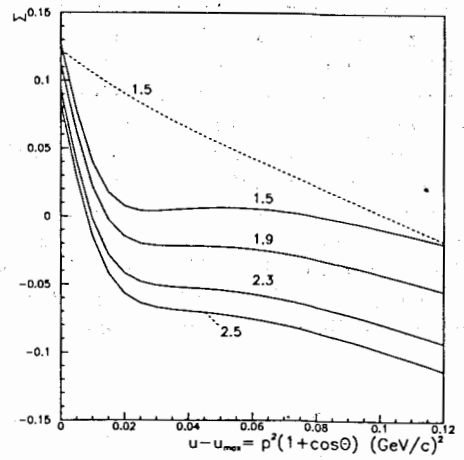

Figure 10: The spin-spin correlation parameter for the process $\vec{p}\ ^3\vec{H}e \to\ ^3Hep$ as a fubction of $|u - u_{max}|$. Full curves show the results of calculations taking into account rescatterings in the initial and final states for different energies of the incident proton (GeV) shown near the curves; the dashed curve is the Born approximation for 1.5 GeV

the fact that the RSC wave function [14] is used here for the ^3He nucleus. The RSC potential provides for the wave functions of the lightest nuclei too intensive high momentum components in comparison with other realistic potentials like the Paris potential (see, for example, [35]).

The numerical results for the parameter Σ obtained with allowance for two channels $\nu = 1$ and $\nu = 2$ in the ^3He wave function are presented in Fig. 10 versus the variable $|u - u_{max}| = 2p^2(1 + \cos\theta_{c.m.})$, where p is the proton momentum in the $p+\ ^3He$ c.m.s. and $\theta_{c.m.}$ is the scattering angle. One can see from this figure that at $\theta_{c.m.} = 180°$ and $T_p \sim 1 - 2.5$ GeV the value Σ is about $\sim 0.1 - 0.15$ independently of the initial energy. Rescatterings in the initial and final states modify the form of angular dependence but do not change the energy dependence at $\theta_{c.m.} = 180°$. The similar behaviour displays the spin averaged cross section [8].

4 Conclusion

The question about a presence of nonnucleon degrees of freedom in the structure of the lightest nuclei at short NN-distances can be reformulated in other words in the following way. Up to what maximal values of relative momenta between nucleons inside a nucleus does the latter demonstrate the properties of the system which consists

of nucleons with frozen internal degrees of freedom interacting by means of realistic NN-potentials defined from the NN-phase shifts data?

In this work the remarkable sensitivity of the cross section of backward elastic $p\,^3He$-scattering to the high momentum components of the ^3He wave function in the S-wave channel is found for energies above 1 GeV. The total dominance of nucleon degrees of freedom in the ^3He nucleus is demonstrated at these kinematical conditions. It is shown that the backward elastic $p\,^3He$-scattering advantageously differs in this respect from the backward elastic pd-scattering. Some arguments are given to show that this feature of the $p\,^3He \to\, ^3Hep$ process is connected with the high momentum component of the ^3He wave function, which is more intensive in comparison with the deuteron wave function. Since the mechanism of the np-pair transfer describes the available experimental data in the interval of incident energies 0.9-1.7 GeV satisfactorily, there is a reason to measure the cross section at higher energies in order to enlighten the validity of phenomenological NN-potentials in describing the structure of lightest nuclei at high relative momenta of nucleons.

Acknowledgements.

I am thankful to Prof. V.I. Komarov for discussions. This work was supported in part by the Russian Foundation for Basic Research (grant N^o 96-02-17215).

Appendix

Here are presented the formulas for the amplitude of the np-pair transfer taking into account the first two channels $\nu = 1,2$ in the ^3He wave function. The function given by Eq.(45) was approximated in [28] by the sum of Yukawa terms. Using the parametrization [28] we found the gaussian parametrization for the functions $f_\nu(p) = \{\phi_\nu(p), \chi_\nu(p)\}$,

$$\varphi(q) = \sum_i G_i \exp(-\alpha_i q^2), \quad \chi(p) = \sum_j F_i \exp(-\beta_i p^2) \tag{48}$$

with the coefficients given in Table 2. These coefficients were found by means the minimization of the difference between the integrals

$$I(\mathbf{Q}) = \int f_\nu(\mathbf{q}) f_\nu(\mathbf{q}+\mathbf{Q}) d\mathbf{q}, \tag{49}$$

calculated in the interval $Q = 0 \div 13 fm^{-1}$ with the functions $f_\nu(p) = \{\phi_\nu(p), \chi_\nu(p)\}$ from Ref. [28] on the one side and with the gaussian parametrization in Eq. (48) on the other side.

Tabl.1 Coefficients for the expansions in Eq. (47)

S_i, $fm^{-3/2}$	κ_i, fm^{-2}	D_i, $fm^{-7/2}$	λ_i, fm^{-2}
1.80112E-02	2.15766 E-02	-1.93862E-03	9.83826 E-02
2.13255E-01	8.35379 E-02	-1.58838 E-02	3.18527 E-01
9.00237E-02	1.27578 E-01	-3.11061 E-02	6.43963 E-01
3.23190E-01	3.26778 E-01	-3.83184 E-02	1.19183 E+00
-2.17017E-01	1.06206 E+00	-9.57312 E-02	4.47721 E+00

Tabl.2 Coefficients for the expansions in Eq. (48)

ν	ϕ_ν		χ_ν	
	G_i, $fm^{\frac{3}{2}}$	α_i, fm^2	F_i, $fm^{\frac{3}{2}}$	β_i, fm^2
1	2.413615	5.535106	4.20690	7.62335
	-1.299993 E-01	1.060713 E-01	2.59354	2.37678
	4.118231 E-02	4.555083 E-03	4.8189 E-01	9.18116 E-01
	1.762614 E-00	1.611916 E+00	-2.45993E-02	1.60613 E-01
	7.491376 E-01	5.466668 E-01	5.21600 E-03	1.40849 E-02
	-4.00000 E-02	4.526665 E-03	-5.67292 E-03	1.03918 E-02
	-3.451822 E-02	5.023824 E-02	2.17920 E-03	7.19787 E-03
2	-2.54039	6.55162	6.51121	9.38385
	-1.93783	1.74914	2.59354	3.04139
	-7.74249 E-01	5.72939 E-01	5.45100 E-01	1.22803
	1.12706 E-01	1.15040 E-01	-2.40357 E-02	1.85314 E-01
	3.09857 E-02	5.11790 E-02	1.56646 E-03	1.84247 E-02
	-6.4000 E-03	3.94752 E-02	-2.61864 E-03	1.03918 E-02
	1.18765 E-03	6.58383 E-03	2.17920 E-03	9.12018 E-03

Using the gaussian parametrization for the functions $\varphi(q)$ and $\chi(p)$ we find the following expression for the integrals in Eq.(12)

$$I(\mathbf{Q}_1, \mathbf{Q}_0) = \frac{1}{(4\pi)^2} \int d^3q (q^2 + M^2) \varphi_{\nu'}(\gamma' \mathbf{q} + \delta' \mathbf{Q}_0) \varphi_\nu(\gamma \mathbf{q} + \delta \mathbf{Q}_1)$$

$$\chi_\nu(a\mathbf{q} + b\mathbf{Q}_1) \chi_{\nu'}(a'\mathbf{q} + b'\mathbf{Q}_0) = \frac{1}{(4\pi)^2} \sum_{i,j,k,l} G_i G_j F_k F_l \left(\frac{\pi}{D}\right)^{3/2}$$

$$\times \left\{ M^2 + D^{-1}\left(\frac{3}{2} + B^2\, D^{-1}\right)\right\} \exp\left[\frac{B^2}{D} - C\right], \qquad (50)$$

where

$$\begin{aligned} C &= \left[\alpha_i(\delta')^2 + \alpha_j\delta^2 + \beta_k b^2 + \beta_l(b')^2\right] Q^2, \\ D &= \alpha_i(\gamma')^2 + \alpha_j\gamma^2 + \beta_k a^2 + \beta_l(a')^2, \\ B^2 &= (\alpha_i\gamma'\beta' + \beta_l a'b')^2\, Q_0^2 + (\alpha_j\gamma\delta + \beta_k ab)^2\, Q_1^2 + \\ &\quad + 2\mathbf{Q_1}\mathbf{Q_0}\,(\alpha_i\gamma'\beta' + \beta_l a'b')\,(\alpha_j\gamma\delta + \beta_k ab)\,, \end{aligned} \qquad (51)$$

In Eq.(50-51) the summation over the indices i, j, k, l refers to the expansions in Eq.(48) for the functions $\varphi_{\nu'}$, φ_ν, χ_ν, $\chi_{\nu'}$, respectively.

From Eq. (7) one finds for the ST mechanism :

$$\begin{aligned} &\gamma' = -\frac{1}{2},\ \delta = -\frac{3}{4};\ \gamma = -\frac{1}{2},\ \delta = \frac{3}{4}, \\ &a' = 1,\ b' = -\frac{1}{2};\ a = -1,\ b = -\frac{1}{2}. \end{aligned} \qquad (52)$$

Therefore, at the scattering angle $\theta_{c.m.} = 180^0$ (*et id.* $\mathbf{Q_1} = -\mathbf{Q_0}$) the expression in the exponent for the ST amplitude in Eq.(50) takes the form

$$\left[\frac{B^2}{D} - C\right]_{ST} = -\mathbf{Q}_0^2 \left\{ \frac{(\alpha_i + \alpha_j)(\beta_k + \beta_l)}{\frac{1}{4}(\alpha_i + \alpha_j) + (\beta_k + \beta_l)} \right\}. \qquad (53)$$

One can find the following three conditions for which the absolute magnitude of the value in the right hand side of Eq.(53) has a minimum at $Q_0 = Q_1 = const$.

A) In the case $\alpha_i + \alpha_j \ll \beta_k + \beta_l \sim 1$ one finds from Eq.(53) the relation $-\frac{1}{\mathbf{Q}^2{}_0}\left[\frac{B^2}{D} - C\right]_{ST} \sim (\alpha_i + \alpha_j)(1 - \frac{1}{4}\frac{\alpha_i+\alpha_j}{\beta_k+\beta_l}) \ll 1$. Due to the relation $\beta_k + \beta_l \sim 1$ the product of pre-exponentials F_kF_l in Eq.(50) is large according to Table 2 which gives the correspondence between β_i and F_i.

B) $\beta_k + \beta_l \ll \alpha_i + \alpha_j \sim 1$. It corresponds to the relation $-\frac{1}{\mathbf{Q}^2{}_0}\left[\frac{B^2}{D} - C\right]_{ST} \sim 4(\beta_k + \beta_l)$.

C) $\beta_k + \beta_l \sim \alpha_i + \alpha_j \ll 1$. In this case one finds $-\frac{1}{\mathbf{Q}^2{}_0}\left[\frac{B^2}{D} - C\right]_{ST} \sim 4(\beta_k + \beta_l)$, however all pre-exponentials G_i, G_j, F_k, F_l in Eq.(50) are small (see Table 2).

It is obvious, that only in the case A) the exponent takes the minimal value which corresponds to the maximal value of the ST amplitude. In this case the first condition $\alpha_i + \alpha_j \ll 1$ means that the high momentum components of two functions $\varphi_{\nu'}(q)$ and $\varphi_\nu(q)$ are involved in the ST-amplitude, whereas the second condition $\beta_k + \beta_l \sim 1$ corresponds to soft momenta ($p \sim 1/\sqrt{\beta_k}$, $1/\sqrt{\beta_l}$) in the other two functions $\chi_{\nu'}(p)$, $\chi_\nu(p)$ [2].

[2]Note that using the harmonic oscillator translationally-invariant shell model wave function for the ^3He nucleus [36] one keeps only one gaussian term in Eqs. (48) with the exponents α and β related as $\beta = \frac{3}{4}\alpha$. In this case the positive term B^2/D in the exponent of Eq.(50), which moderates the decrease of the amplitude with increasing Q_0, vanishes for the ST mechanism ($B^2/D = 0$). As a result, the ST mechanism reduces to the deuteron exchange mechanism.

Similarly, one can find for the NST mechanism :

$$\begin{aligned} &\gamma' = -\frac{1}{2},\ \delta = -\frac{3}{4};\ \gamma = -\frac{1}{2},\ \delta = -\frac{3}{4}, \\ &a' = 1,\ b' = -\frac{1}{2};\ a = 1,\ b = -\frac{1}{2}. \end{aligned} \qquad (54)$$

$$-\frac{1}{\mathbf{Q}_0^2}\left[\frac{B^2}{D} - C\right]_{NST} = \left\{ \frac{(\alpha_i + \alpha_j)(\beta_k + \beta_l) + \left[\frac{3}{2}\alpha_i\alpha_j + 2\beta_k\beta_l\right]}{\frac{1}{4}(\alpha_i + \alpha_j) + (\beta_k + \beta_l)} \right\}. \qquad (55)$$

Due to an additional term in the square brackets in the numerator on the right hand side of Eq. (55) the exponent for the NST mechanism is always larger in absolute value than the exponent for the ST mechanism. For this reason the contribution of the NST mechanism to the cross section is considerably smaller in comparison with the ST mechanism.

The IPT amplitude is defined by the integral in Eq. (50) under the following conditions [8]

$$\begin{aligned} &\gamma' = 1,\ \delta' = 0;\ \gamma = -\frac{1}{2},\ \delta = \frac{3}{4}, \\ &a' = 0,\ b' = 1;\ a = -1,\ b = -\frac{1}{2}; \end{aligned} \qquad (56)$$

$$-\frac{1}{\mathbf{Q}_0^2}\left[\frac{B^2}{D} - C\right]_{IPT} = \left\{ \beta_l + \frac{\alpha_j\left(\beta_k + \frac{9}{4}\alpha_i\right) + \frac{1}{4}\alpha_i^2}{\alpha_i + \frac{1}{4}\alpha_j + \beta_k} \right\}. \qquad (57)$$

It is easy to find that the minimum of the right-hand side in Eq.(57) takes place for $\beta_l \ll 1$, $\alpha_i \ll \beta_k$, $\alpha_j \ll \beta_k$. This means that the main contribution to the IPT amplitude comes from the high momentum components of three functions $\chi_{\nu'}$, $\varphi_{\nu'}$ and φ_ν simultaneously.

References

[1] V.M. Kolybasov and N.Ya. Smorodinskaya, Yad. Fiz. 17 (1973) 1211.

[2] L.A. Kondratyuk, F.M. LeV and L.V. Shevchenko, Yad. Fiz. 29 (1979) 1081; Yad. Fiz. 33 (1981) 1208.

[3] A. Boudard and M.Dillig, Phys. Rev. C31 (1985) 302.

[4] A.Nakamura and L.Satta, Nucl.Phys. A445 (1985) 706.

[5] Yu. N. Uzikov, Phys. At. Nucl. 60 (1997) 1458.

[6] L.P. Kaptari, B.kämpfer, S.M. Dorkin and S.S. Semikh, Phys.Rev. C57 (1998) 1097 .

[7] A.V. Lado and Yu.N. Uzikov, Phys. Lett. B279(1992) 16.

[8] L.D. Blokhintsev, A.V. Lado and Yu.N. Uzikov, Nucl.Phys. A597 (1996) 487.

[9] S.A. Gurvitz, Phys. Rev. C 22 (1980) 964.

[10] M.A. Zhusupov, Yu.N. Uzikov and G.A. Yuldasheva, Izv. AN KazSSR ser. fiz.-mat., N6 (1986) 69.

[11] M.S. Abdelmonem and H.S. Sherif, Phys. Rev. C 36 (1987) 1900.

[12] M.I. Paez and R.H. Landau, Phys. Rev. C29 (1984) 2267.

[13] R.H. Landau and M. Sagen, Phys. Rev. C 33 (1986) 447.

[14] R.A. Brandenburg, Y.Kim and A. Tubis, Phys. Rev. C12 (1975) 1368.

[15] P. Berthet et al., Phys. Lett. B106 (1981) 465.

[16] A.V. Lado and Yu.N. Uzikov, Izv.RAN SSR 57 (1993) 122.

[17] V.V.Burov et al., Z.Phys. A306 (1982) 149.

[18] S.I. Bylenkaya, Yu.M. Kazarinov and L.I. Lapidus, JETP 60 (1971) 460.

[19] R.G. Arnold et al., Phys.Rev.Lett. 40 (1978) 1429.

[20] R. Schiavilla, V.R.Pandaripande and R.B. Wiringa, Nucl. Phys. A449 (1986) 219.

[21] F.D.Santos, A.M. Eiro and A. Barosso, Phys.Rev. C19 (1979) 238.

[22] B.F. Gibbson and D.R. Lehman, Phys.Rev. C29 (1984) 1017.

[23] O. Imambekov and Yu. N. Uzikov, Yad. Fiz. 47 (1988) 1089.

[24] A. Matsuyama and T.-S. H. Lee, Phys.Rev. C34 (1986) 1900.

[25] A.G. Sitenko. Fiz. Elem. Chast. At. Yadra. 4 (1973) 547.

[26] Particle Data Group Report UCRL 20000 NN.1979.

[27] W.Cziz and L.Lesniak, Phys.Lett. B24 (1967) 227.

[28] Ch. H. Haiduk, A. M.Green and M.E. Sainio, Nucl.Phys. A337 (1980) 13.

[29] G. Alberi, L.P. Rosa and Z.D. Thome, Phys.Rev.Lett. 34 (1975) 503.

[30] P.Berthet et al., Nucl.Phys. A443 (1985) 589.

[31] L.S. Azhgirey et al., Phys.Lett. B391 (1997) 22.

[32] A. Boudard, These, CEA-N-2386, Saclay, (1984).

[33] P.Berthet et al., J.Phys.G: Nucl.Phys. 8 (1982) L111.

[34] L. Dubal et al., Phys. Rev. D9 (1974) 597.

[35] O.Imambekov, Yu.N. Uzikov and L.V. Shevchenko, Z.Phys. A332 (1989) 349.

[36] V.G. Neudatchin and Yu.F. Smirnov. Nuclonnie associacii v legkich yadrach (Moskwa, Nauka, 1969) p. 410.

Received by Publishing Department
on October 13, 1998.

Узиков Ю.Н. E2-98-287

Структура ядра ^{3}He в упругом p ^{3}He-рассеянии назад

Исследовано упругое p ^{3}He-рассеяние назад при кинетической энергии налетающего протона $T_p > 1$ ГэВ в рамках механизмов обмена np-парой и треугольной диаграммы однопионного обмена с подпроцессом $pd \to {}^3\mathrm{He}\,\pi^0$ на основе использования реалистической трехтельной волновой функции для ядра ^{3}He. Показано, что механизм передачи np-пары доминирует, а экспериментально наблюдаемое сечение рассматриваемого процесса при $T_p > 1$ ГэВ определяется, главным образом, значениями фаддеевской компоненты волновой функции ядра ^{3}He, $\varphi^{23}(q_{23}, p_1)$ при больших относительных импульсах $q_{23} > 0{,}6$ ГэВ/с NN-пары в $^1S_0$-состоянии и малых импульсах «спектатора» $p_1 \le 0{,}1$ ГэВ/с. В рамках доминирующего механизма вычислен параметр спин-спиновой корреляции для процесса рассеяния с поляризованным пучком и мишенью. Учтены перерассеяния в начальном и конечном состояниях. Проведено сравнение с процессом $pd \to dp$, которое показывает, что доминирующая роль механизма передачи np-пары обусловлена высокоимпульсной компонентой волновой функции ядра ^{3}He.

Работа выполнена в Лаборатории ядерных проблем ОИЯИ.

Препринт Объединенного института ядерных исследований. Дубна, 1998

Uzikov Yu.N. E2-98-287

Structure of the ^{3}He in Backward Elastic p ^{3}He-Scattering

Backward elastic p ^{3}He-scattering at incident proton kinetic energies $T_p > 1$ GeV is investigated in the framework of the np-pair transfer mechanism and triangular diagram of one-pion exchange with a subprocess $pd \to {}^3\mathrm{He}\,\pi^0$ using a realistic three-body wave function of the ^{3}He nucleus. It is found that the np-pair transfer mechanism dominates owing to a rich high momentum component of the ^{3}He wave function. We show that the experimental cross section of this process is defined mainly by the values of the Faddeev component of the ^{3}He wave function, $\varphi^{23}(q_{23}, p_1)$, at high relative momenta $q_{23} > 0.6$ GeV/c of the NN-pair in the $^1S_0$-state and at low spectator momenta $p_1 \le 0.1$ GeV/c. The spin-spin correlation parameter is calculated in the framework of the dominating mechanism for the case of polarized target and beam. Rescatterings in the initial and final states are taken into account. Comparison with the $pd \to dp$ process is performed.

The investigation has been performed at the Laboratory of Nuclear Problems, JINR.

Preprint of the Joint Institute for Nuclear Research. Dubna, 1998